Polymer Chemistry

Accepted Manuscript

ROYAL SOCIETY OF CHEMISTRY

www.rsc.org/polymers

Journal Name

RSCPublishing

ARTICLE

Probing the dendritic architecture through AIE: challenges and successes

Cite this: DOI: 10.1039/x0xx00000x

Mathieu Arseneault,[†] Nelson L. C. Leung,[†] Lai Tsz Fung,[†] Rongrong Hu,[†] Jean-François Morin[£] and Ben Zhong Tang[*, †, ‡, §]

Received 00th January 2012,
Accepted 00th January 2012

DOI: 10.1039/x0xx00000x

www.rsc.org/

Since the aggregation-induced emission (AIE) phenomenon is very sensitive to steric hindrance, we set out to use it as a tool to probe the periphery of dendrimers. To achieve this, dendrimers with an ethylene oxide (EO) core were synthesized and then decorated with AIE-active units. Tetraphenylethylene (TPE) with varying spacer lengths was used as the AIE decoration to create two parallel series of these dendrimers up to generation four. Systematic photoluminescence studies demonstrated that peripheral crowding starts at G3. Further analysis showed that the AIE technique is sensitive enough to distinguish small differences in architecture. When used in combination with Dynamic Light Scattering, our AIE strategy revealed a complex relationship between the aggregates size and their emission.

1. INTRODUCTION

The aggregation induced emission (AIE) phenomenon pertains to fluorogens whose emission is turned on in the aggregated state rather than in a dilute solution. Prior to the introduction of AIE in 2001[1], it was common knowledge that aggregation was detrimental to the emission of organic fragments due to non-radiative excited energy transfers.[2-4] This is still true for conventional fluorogens that are highly-conjugated and planar.[5-7] Inversely, AIE-active molecules dissipate their energy through non-radiative channels in the solution state and show little to no emission. Once the molecules aggregate, these channels are blocked and the excitation energy is dissipated through emerging radiative channels, thus behaving the exact opposite way than their conventional counterparts. The AIE concept has been incorporated in a plethora of systems over the last decade.[8-11] Most of these reports focus on harnessing the solid-state and "turn on" features of AIE moieties. A smaller fraction of the literature is dedicated to the underlying mechanism driving AIE.[10, 12-14] Thus far, the mechanism put forward by Tang's group is the prevailing one. The beneficial effect of aggregation on fluorescence emission is explained by a restriction of intramolecular rotations (RIR). The confined and constricted molecule that was dissipating its excitation energy through these rotations is now dissipating it through a radiative channel. Seeing how this phenomenon is so sensitive to steric hindrance, we thought it could be used as a tool to probe large molecular structures. By decorating a macromolecule with AIE-active moieties, conformational realities could be investigated. If a proposed conformation change is indeed true under a given stimuli, then the steric environment around the AIE decorations would change, leading to a change of emission. To the best of our knowledge, no work using this strategy with AIE has been reported yet. As a field test for this idea, we set out to probe the steric hindrance at the periphery of a dendritic architecture. Dendrimers are known to have several unique advantages that set them apart from other polymeric architectures.[15-17] Here, their discrete nature is the key feature we sought. By synthesizing consecutive series of dendrimers and then decorating their terminal groups with AIE-active moieties, one could study at which generation the periphery becomes crowded. As shown at the top of Figure 1, when the dendrimer increases in generation, the AIE units will get closer and closer until they aggregate and start emitting. Beyond intrinsic conformation probing, this strategy could also help unravel stimuli-induced conformation changes as the AIE decorations respond to the movements of the dendrimers. This is reminiscent of the fluorescence emission from the jellyfish. As it breathes, molecular changes lead to fluorescence. This phenomenon can be mimicked as demonstrated by Zhu et al. in 2012.[18] While their system is

†Department of Chemistry, ‡Institute for Advanced Study, State Key Laboratory of Molecular Neuroscience, Institute of Molecular Functional Materials and Division of Life Sciences, The Hong Kong University of Science and Technology (HKUST), Clear Water Bay, Kowloon, Hong Kong, China, E-mail: tangbenz@ust.hk
£Département de chimie and Centre de Recherche sur les Matériaux Avancés (CERMA), 1045 Ave de la Médecine, Université Laval, Québec, Canada G1V 0A6
‡Guangdong Innovative Research Team, SCUT-HKUST Joint Research Laboratory, State Key Laboratory of Luminescent Materials and Devices, Institute of South China University of Technology (SCUT), Guangzhou, China, 510640
§HKUST Shenzhen Research Institute, No. 9 Yuexing 1st RD, South Area, Hi-tech Park, Nanshan, Shenzhen, China 518057.

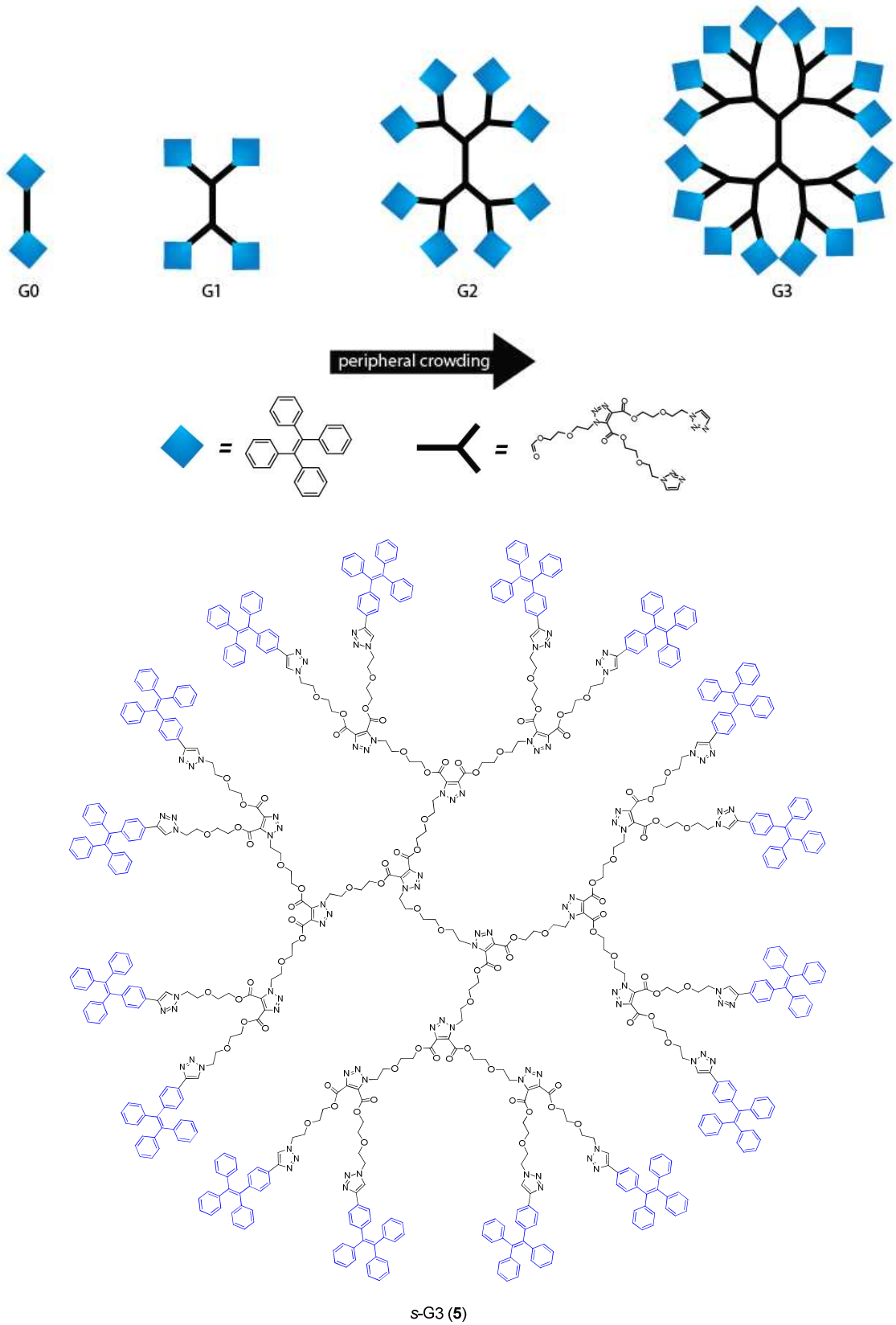

s-G3 (**5**)

Fig. 1 Peripheral crowding occurring as the generation increase (A) and s-G3 (5) (B)

triggered mainly by pH, our method could be used with any kind of stimuli such as pH, ionic forces, temperature, precipitation, etc. To realize our proof-of-concept, we first needed to synthesize a series of dendrimers and decorate each generation with AIE-active moieties. Interestingly, very few AIE-active dendrimers have been reported so far.[19-24] The examples we found in the literature fall into two broad categories: those with an AIE core[19, 20] and those decorated with AIE-moities.[21-24] When considering the dendrimers bearing AIE-gens on their termini, none went above G2 and therefore the issue of steric hindrance has not been fully explored yet. Hyperbranched polymers decorated with tetraphenylethylene (TPE) units have also been synthesized and are reported to have some background emission.[25-31] Their polydispersity makes it hard if not impossible to systematically study the differences between structures.

In light of all this, the architecture reported by Morin *et al.*[32] was chosen as shown in Scheme 2. Its ethylene oxide (EO) branches give it high solubility in most organic solvents. Moreover, its terminal groups are azide, making them ready for a copper alkyne-azide coupling (CuAAC). TPE was chosen as the AIE decoration on account of its flexible synthesis and because it is devoid of groups that could interfere with synthetic conditions. Scheme 1 summarizes our global synthetic approach.

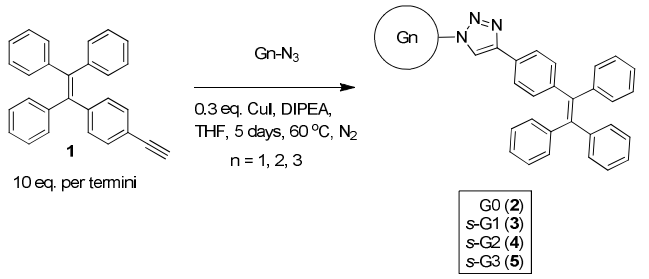

Scheme 1 The synthetic strategy to decorate the EO3-EO2 dendritic core. "s" stands for "short"

While successful, our initial attempts revealed difficulties preventing us from reaching G4. Very low yields pushed us to develop an alternative route. This second approach involves the use of a click-activating spacer between the TPE and the dendrimer. This resulted in two different series of dendrimers with varying steric hindrance at the periphery. G4 was obtained with a conversion rate nearing 95 %, making it possibly the largest AIE-dendrimer yet. Herein, we report their synthesis as well as their photoluminescence behaviour. We observed several interesting trends that we analyse here, the main one being that peripheral crowding occurs at G3. Subtle differences between architectures could also be observed. Thus, colloid and polymer chemistry will benefit from this approach to answer fundamental conformation questions.

Experimental

Materials and instruments

THF (VWR) was distilled from sodium benzophenone ketyl under nitrogen immediately prior to use. Other solvents were purchased from VWR or BDH and were used without further purification. All other reagents were purchased from Aldrich and used without further purification.

Polydispersity (M_w/M_n) of the dendrimers were measured by a Waters gel permeation chromatography (GPC) system equipped with a Waters 515 HPLC pump, a set of Waters Styragel columns (HT3, HT4, and HT6 with molecular weight range of 10^2–10^7), a column temperature controller, a Waters 486 wavelength-tunable UV–vis detector, a Waters 2414 differential refractometer and a Waters 2475 fluorescence detector. The dendrimer samples were freshly prepared by dissolving in THF (2 mg/mL) and then filtering through 0.45 µm PTFE syringe-type filters before being injected into the GPC system. THF was used as the mobile phase at a flow rate of 1.0 mL/min. The column temperature and the wavelength of the UV-vis detector were set at 40 °C and 254 nm, respectively. Monodispersed polystyrene standards (Waters) covering the molecular weight range of 10^3–10^7 were used for the calibration.

^{1}H and ^{13}C NMR spectra were measured on Bruker ARX 300 NMR and Bruker ARX 400 NMR spectrometers using or CDCl3 as the deuterated solvent and tetramethylsilane (TMS; δ = 0 ppm) as the internal standard. UV-vis absorption spectra were measured on a Milton Roy Spectronic 3000 array spectrophotometer. Photoluminescence (PL) spectra were recorded on a Perkin-Elmer spectrofluorometer LS 55. IR spectra were recorded on a Perkin-Elmer 16 PC FT-IR spectrophotometer. MALDI–TOF mass spectra were recorded on a GCT premier CAB048 mass spectrometer or on a MALDI TOF/TOF ultrafleXtreme mass spectrometer. Dynamic light scattering (DLS) measurements were recorded on a zeta potential analyser ZetaPAL from Brookhaven Instruments (USA) alongside version 2.4.1 of the corresponding software. A quartz cell with an optical pathway of 1 cm was used. Unless indicated otherwise, all measurements were done in pure THF at a concentration of 2 x 10^{-5} M and filtered through a PTFE 0.45 µm filter right before acquisition.

Photoluminescence measurements

Unless otherwise stated, all photoluminescence (PL) measurements were performed at a concentration of 1 x 10^{-5} M. Freshly distilled THF was used alongside deionized water and HPLC grade acetonitrile (ACN). Our typical procedure starts by putting 100 µL of a dendrimer stock solution (10^{-3} M) in a 10 mL volumetric flask. The appropriate volume of THF was added and the flask shaken on a bench top vortex. The flask was filled with water with additional shaking between each mL of water. This suspension was used immediately in a quartz cell with a 1 cm optical pathway for all PL measurements. The excitation wavelength was 327 nm for all samples.

Synthesis of dendrimer cores

Synthesis was repeated from the reported procedure with similar yield and purity for G1 to 3.[32]

Synthesis of EO3-EO2-G4-I (14)

Following the same procedure than for earlier generations, EO3-EO2-G3-N_3 (**13**) (0.500 g, 1.01 x 10^{-4} mol., 1 eq.) was carefully mixed with the branching synthon (**7**) (0.822 g, 1.61 x 10^{-3} mol., 16 eq.) as dry oils in a precise ratio of 1:1 for each azide termini in a 10 mL round bottom flask. A stir bar and chloroform (2 mL) were added. The flask was then mounted with a condenser and purged with nitrogen 3 times. The reaction was heated at 70 °C for 1 night. The flask was put directly on a rotary evaporator for an hour to remove the chloroform. Yield is quantitative for 1.322 g, 1.01 x 10^{-4} mol. as an amber-colored oil. ^{1}H NMR ($CDCl_3$, 400 MHz): ^{13}C NMR (CDCl3, 400 MHz): δ 159.86 (s), 158.30 (s), 71.99 – 71.88 (m), 71.64 (s), 69.04 (s), 68.33 (s), 67.96 (d, J = 6.0 Hz), 65.76 – 65.65 (m), 64.54 (t, J = 14.8 Hz), 50.20 (s). IR (NaCl): 2912, 1732, 1553, 1464, 1275, 1205, 1128, 1065, 910 ν cm^{-1}. HRMS: Could not be obtained due to the limitation of our apparatus.

Synthesis of EO3-EO2-G4-N_3 (15)

Following the same procedure than for earlier generations, EO3-EO2-G4-I (**14**) (1.322 g, 1.01 x 10^{-4} mol., 1 eq.) was dissolved in DMF (10 mL) in a 50 mL round bottom flask equipped with a stir bar and a condenser. Sodium azide (0.420 g, 64.4 x 10^{-3} mol., 64 eq.) was added and the reaction was stirred at 75 °C for 24 h. After being cooled to room temperature, the mixture was diluted in 50 mL of ethyl acetate. This organic layer was then washed eight times with a solution of NaCl to remove the DMF. The organic layer was then dried over $MgSO_4$ before being filtered and evaporated. This evaporation was monitored by ^{1}H NMR to verify that there was no solvent left. Yield is 85 % for 0.888 g, 1.01 x 10^{-4} mol as an amber-colored oil. ^{1}H NMR (400 MHz, $CDCl_3$) δ 4.83 (m), 4.62 – 4.30 (m), 4.03 – 3.59 (m), 3.46 – 3.33 (m), see image in SI. ^{13}C NMR (400 MHz, $CDCl_3$) δ 70.05 (s), 68.76 (s), 68.46 – 68.22 (m), 65.89 – 65.16 (m), 64.79 – 64.37 (m), 50.65 (s), 50.05 (s). IR (NaCl): 2964, 2876, 2824, 2108, 1734, 1553, 1466, 1279, 1205, 1128, 1066 ν cm^{-1}. HRMS: Could not be obtained due to the limitation of our apparatus.

Synthesis of compound G0 (2)

Compound **1** (0.700 g, 1.97 x 10^{-3} mol., 2.5 eq.) and compound **6** (0.157 g, 0.79 x 10^{-3} mol., 1 eq.) were dissolved in THF and MeOH (5 mL each). DIPEA (0.4 mL) and CuI (0.150 g, 0.79 x 10^{-3} mol., 1 eq.) were added and the mixture was stirred at room temperature for 48 h before being condensed under vacuum. It was then extracted with DCM and a brine of NH_4Cl three times. The organic layer was then dried over $MgSO_4$ and evaporated. The substrate was purified over column chromatography (1:1 DCM : hexanes, first band). A yellow powder was collected with a yield of 71 % (0.506 g, 0.56 x 10^{-3} mol.). ^{1}H NMR (400 MHz, CDCl3) δ 7.74 (s, 1H), 7.54 (d, *J* = 8.3 Hz, 1H), 7.04 (ddt, J = 9.8, 6.1, 2.8 Hz, 9H), 4.42 (t, *J* = 5.0 Hz, 1H), 3.78 (t, *J* = 5.0 Hz, 1H), 3.51 (s, 1H). ^{13}C NMR (400 MHz, $CDCl_3$) δ 147.44 (s), 144.06 – 143.35 (m), 141.32 (d, *J* = 1.4 Hz), 140.42 (s), 131.93 (d, *J* = 3.5 Hz), 131.32 (t, J = 6.3 Hz), 128.56 (d, *J* = 1.7 Hz), 127.72 (dd, *J* = 11.0, 4.0 Hz), 126.81 – 126.09 (m), 124.96 (d, *J* = 2.7 Hz), 120.91 (s), 103.83 (s), 70.41 (d, *J* = 3.3 Hz), 69.46 (d, *J* = 3.4 Hz), 66.99 (s), 66.45 – 65.46 (m), 50.25 (d, *J* = 4.5 Hz), 41.12 (s), 32.33 (s), 23.47 (s), 22.68 (s). IR (NaCl): 3142, 3055 (t), 2876 (br), 2725, 2245, 1952, 1724, 1599, 1493, 1443, 1360, 1227, 1115, 1074, 910 ν cm^{-1}. HRMS: calcd. 913.1153 found 913.4219

Synthesis of *s*-G1 (3)

EO3-EO2-G1-N_3 (**9**) (0.130 g, 1.48 x 10^{-4} mol., 1 eq.) was dissolved in THF (3 mL), compound 1 (0.631 g, 1.78 x 10^{-3} mol., 12 eq.) and DIPEA (100 µL) in a 2 neck round-bottom flask equipped with a condenser. The flask was purged with nitrogen before adding CuI (0.113 g, 5.93 x 10^{-4} mol., 4 eq.). The mixture was refluxed for five days before being cooled to room temperature. The solvent was evaporated and the resulting dark yellow solid was dissolved in DCM. It was then washed with saturated NH_4Cl until the aqueous layer stayed uncolored for two consecutive washes. After being dried and evaporated, the organic layer was passed on a chromatography column. It was first flushed in pure hexanes to remove the bulk of compound 1 and then in $CHCl_3$ to remove a red band. Finally, the desired dendrimer was recuperated by carefully eluting with the addition of 3% MeOH into $CHCl_3$ in a 27 % yield (0.092 g, 3.99 x 10^{-5} mol.) as a pale yellow solid. 1H NMR (400 MHz, $CDCl_3$): δ 7.86 (s, 2H), 7.79 (s, 2H) 7.55 (d, J = 8.4 Hz, 4H), 7.49 (d, J = 8.1 Hz, 4H), 7.05 (m, 68H), 4.53 (t, J = 5.3 Hz, 4H), 4.48 (t, J = 5.3 Hz, 4H), 4.41 (m, 4H), 3.85 (dd, J = 5 Hz, 8H), 3.57 (t, J = 5.2Hz, 8H), 3.25 (s, 4H). 13C NMR (400 MHz, $CDCl_3$): 159.83, 158.16, 147.54, 147.42, 143.79, 143.61, 141.37, 141.29, 140.44, 140.35, 139.43, 131.87, 131.80, 131.37, 128.63, 128.42, 127.75, 126.57, 125.01, 124.81, 120.89, 120.76, 70.16, 69.53, 69.23, 69.03, 68.82, 68.49, 65.11, 64.40, 50.26, 50.16, 49.95. IR (NaCl): 3053 (br t), 2916 (br t), 1734, 1597, 1555, 1493, 1442, 1273, 1209, 1128, 1074 ν cm^{-1}. MS: calcd. 2306.61, found 2307.1

Synthesis of s-G2 (4)

EO3-EO2-G2-N_3 (**11**) (0.150 g, 6.69 x 10-5 mol., 1 eq.) was dissolved in THF (6 mL), compound 1 (2.00 g, 5.65 x 10^{-3} mol., 84 eq.) and DIPEA (200 µL) in a 2 neck round-bottom flask equipped with a condenser. The flask was purged with nitrogen before adding CuI (0.150 g, 7.87 x 10^{-4} mol., 12 eq.). The mixture was refluxed for five days before being cooled to room temperature. At that point, most of the solvent had dried away, leaving a brown solid that was dissolved in DCM. It was then washed with saturated NH_4Cl until the aqueous layer stayed uncoloured for two consecutive washes. After being dried and evaporated, the organic layer was passed on a chromatography column. It was first flushed in pure DCM to remove the bulk of compound 1 and then in $CHCl_3$ to remove a red band. Finally, the desired dendrimer was recuperated by eluting with the addition of 3 % MeOH into $CHCl_3$. After evaporation, the yield is 39 % (0.132 g, 2.59 x 10^{-5} mol.) as a brown solid. ^{1}H NMR (400 MHz, $CDCl_3$): δ 7.89 (d, J = 3.3 Hz), 7.87 (d, J = 3.6 Hz), 7.81 (s), 7.59 – 7.49 (m), 7.07 (dd, J = 4.2 Hz), 4.69 (s), 4.62 (d, J = 4.6 Hz), 4.49 (d, J = 13.0 Hz,), 4.42 (s), 4.33 (dd, J = 6.8), 3.86 (d, J = 11.2 Hz), 3.73 (d, J = 3.8 Hz), 3.63 (s), 3.59 (d, J = 3.5 Hz), 3.46 (d, J =

12.9 Hz), 3.38 (s). ^{13}C NMR ($CDCl_3$, 400 MHz): 159.75 (s), 158.25 (s), 158.15 (s), 147.51 (d), 143.80 (d), 143.60 (s), 141.35 (dd), 140.38 (dd), 139.45 (s), 131.87 (s), 131.80 (s), 131.33 (m), 127.75 (m), 126.59 (m), 125.00 (s), 124.81 (s), 120.92 (m), 68.95 (m), 65.19 (s), 64.38 (s), 50.20 (m), 29.72 (m). IR (NaCl): 3055 (br t), 2922 (br t), 1734, 1597, 1555, 1492, 1442, 1274, 1209, 1128, 1064 ν cm^{-1}. MS: calcd. 5093.62, found 5159.2 (M + Cu)

Synthesis of *s*-G3 (5)

EO2-EO3-G3-N_3 (**11**) (0.100 g, 2.02 x 10-5 mol., 1 eq.) was dissolved in THF (3 mL), compound **1** (1.14 g, 3.22 x 10^{-3} mol., 160 eq.) and DIPEA (200 µL) in a 2 neck round-bottom flask equipped with a condenser. The flask was purged with nitrogen before adding CuI (0.306 g, 1.61 x 10^{-3} mol., 80 eq.). The mixture was refluxed for five days before being cooled to room temperature. The solvent was evaporated and the resulting brown solid was dissolved in DCM. It was then washed with saturated NH_4Cl until the aqueous layer stayed uncoloured for two consecutive washes. After being dried and evaporated, the organic layer was passed on a chromatography column. It was first flushed in pure hexanes to remove the last traces of compound **1** and then in DCM to recuperate the final dendrimer in a 9 % yield (0.020 g, 1.81 x 10^{-6} mol.) as a brown solid. ^{1}H NMR (400 MHz, $CDCl_3$) δ 7.87 (s), 7.70 (d), 7.53 (s), 7.05 (s), 4.76 – 4.22 (m), 3.94 – 3.29 (m). IR (NaCl): 3055, 2928 (br t), 1732, 1599, 1555, 1462, 1365, 1280, 1217, 1128, 1074 ν cm^{-1}. MS: calcd. 10660.2, found 10724.2 (M + Cu)

Synthesis of compound 1 and 16

Synthesis was repeated from the reported procedure with similar yield and purity for compounds 1[25] and 16[33].

Synthesis of compound 17

Compound **9** (1.000 g, 2.81 x 10^{-3} mol., 1 eq.) and compound **12** (0.442, 3.37 x 10^{-3} mol., 1.2 eq.) were mixed in a 25 mL round bottom flask equipped with a stir bar. DIPEA (0.5 mL, ca. 1 eq.), THF (5 mL) and MeOH (5 mL) were added. The flask was then purged with nitrogen before adding CuI (0.267 g, 1.40 x 10^{-3} mol, 0.5 eq.) and K_2CO_3 (ca. 0.5 g, enough to raise the pH around 10). The reaction was stirred at room temperature under nitrogen for one night. An excess of acetylene dicarboxylic acid (0.321 g, 2.81 x 10^{-3} mol., 1 eq.) was added and the reaction was stirred for an additional five minutes. The bulk of the solvent was then evaporated under reduced pressure. The resulting paste was extracted with DCM and water first, then with saturated ammonium chloride three to five times or until two consecutive aqueous layers appeared completely colorless. 1 eq. of acetylene dicarboxylic acid and 2 eq. of K_2CO_3 were added into the organic layer. This mixture was extracted with water. This was done to remove the excess of OH-PEG-N_3 (**12**) that can co-elute with the target compound. This procedure was repeated once. The organic layer was then further washed with water one time. After being dried on $MgSO_4$ and evaporated, the organic layer was purified by column chromatography (100% chloroform, 3rd band), yielding a white flaky solid (1.110 g, 2.28 x 10^{-3} mol, 81 %) ^{1}H NMR (400 MHz, $CDCl_3$) δ 7.83 (s, 1H), 7.57 (d, *J* = 8.3 Hz, 2H), 7.18 – 6.96 (m, 17H), 4.64 – 4.49 (m, 2H), 3.98 – 3.85 (m, 2H), 3.81 – 3.66 (m, 2H), 3.61 – 3.52 (m, 2H). ^{13}C NMR ($CDCl_3$, 400 MHz): δ 143.65 (m), 131.86 (s), 131.37 (d, *J* = 5.5 Hz), 127.90 – 127.56 (m), 126.70 – 126.34 (m), 125.03 (s), 120.61 (s), 77.37 (s), 77.05 (s), 76.73 (s), 72.53 (s), 69.41 (s), 61.69 (s), 50.31 (s). IR (NaCl): 3040, 3053, 2870 (br), 1599, 1493, 1443, 1356, 1227, 1126, 1074, 975 ν cm^{-1}. HRMS: calcd. 487.2260, found 487.2265

Synthesis of compound 19

Compound **17** (05.00 g, 1.03 x 10^{-3} mol, 1 eq.), propiolic acid (**18**) (0.127 mL, 2.05 x 10^{-3} mol., 2 eq.) and PTSA (0.214 g, 1.13 x 10^{-3} mol., 1.1 eq.) were all dissolved in chloroform (8 mL) in a 25 mL round bottom flask with a stir bar. The reaction was refluxed for one night. $NaHCO_3$ (0.5 g) was added to quench the reaction. It was then extracted with DCM and water before being dried over $MgSO_4$ and evaporated. The substrate was purified over column chromatography (pure DCM, first band). A yellow powder was collected with a yield of 52 % (0.290 g, 0.50 x 10^{-3} mol). ^{1}H NMR (400 MHz, $CDCl_3$) δ 7.88 (s, 1H), 7.65 – 7.57 (d J = 8.1 Hz, 2H), 7.15 – 6.97 (m, 17H), 4.61 – 4.54 (t, *J* = 5.0, 2H), 4.37 – 4.32 (t, *J* = 4.4, 2H), 3.89 – 3.82 (t, *J* = 5.0, 2H), 3.71 – 3.65 (t, *J* = 4.4, 2H), 2.55 (s, 1H). ^{13}C NMR (400 MHz, $CDCl_3$) δ 152.55 (s), 147.49 (s), 143.68 (dd, *J* = 9.8, 6.8 Hz), 141.25 (s), 140.58 (s), 131.82 (s), 131.37 (d, *J* = 3.8 Hz), 128.86 (s), 128.14 – 127.55 (m), 126.64 (d, *J* = 5.7 Hz), 125.23 (s), 121.11 (s), 76.08 (s), 74.34 (s), 69.37 (s), 68.55 (s), 64.70 (s), 50.22 (s). IR (NaCl): 3055, 2924, 2851, 2154, 1715, 1647, 1599, 1510, 1445, 1227, 1167, 1117, 841 ν cm^{-1}. HRMS: cald. 540.2242 found 540.2289

General procedure for the TPE-decorated dendrimers (long version)

EO3-EO2-Gn-N_3 (n = 1, 2, 3, 4) was mixed with compound **19** in a ratio of 1 : 1 with each termini in a two-neck 25 mL round-bottom flask equipped with a condenser. THF (2 to 4 mL) and DIPEA (1 eq. per termini) were added and a stream of nitrogen was bubbled for 20 minutes to degas the solution. Copper Iodide (0.5 eq. or 1 eq. per termini) was added and the mixture was then refluxed for 24 h under N_2. It was then cooled to room temperature before being extracted with a DCM/NH_4Cl sat. system at least three times. The organic layer was then dried over $MgSO_4$ and evaporated. No further purification was needed.

Synthesis of *l*-G1 (20)

EO3-EO2-G1-N_3 (**9**) (0.116 g, 1.32 x 10^{-4} mol., 1 eq.), compound **19** (0.285 g, 5.28 x 10^{-3} mol., 4 eq.), CuI (0.050 g, 2.64 x 10^{-4} mol., 2 eq.) and DIPEA (90 µL, 5.28 x 10^{-4} mol., 4 eq.) were used following the general procedure described above. The obtained yield is 72% (0.285 g, 0.95 x 10^{-4} mol.) as yellow translucent flakes. ^{1}H NMR (400 MHz, $CDCl_3$) δ 8.22 – 8.11 (m, 4H), 7.87 (d, J = 17.0 Hz, 4H), 7.56 (d, J = 21.0, 8.1 Hz, 12H), 7.18 – 6.92 (m, 68H), 4.80 (d, J = 18.2 Hz, 2H), 4.68 (t, J = 4.9 Hz, 4H), 4.54 (d, J = 2.6 Hz, 8H), 4.48 – 4.32 (m, 22H), 3.90 (m, 8H), 3.81 (m, 10H), 3.80 – 3.63 (m, 22H), 3.38 (m, 4H). ^{13}C NMR ($CDCl_3$, 400 MHz):

149.05 (s), 143.61 (s), 131.78 (s), 131.31 (d), 127.73 (m), 126.50 (m), 124.98 (s), 120.89 (s), 68.73 (s), 63.54 (s), 49.95 (m). IR (NaCl): 3142, 3055 (t), 2874 (br), 1950, 1722, 1599, 1493, 1443, 1358, 1227, 1111, 910 ν cm^{-1}. HRMS: cald. 3037.2 found 3037.8

Synthesis of *l*-G2 (21)

EO3-EO2-G2-N_3 (**11**) (0.139 g, 6.20 x 10^{-5} mol., 1 eq.), compound **19** (0.267 g, 4.96 x 10^{-4} mol., 8 eq.), CuI (0.094 g, 4.94 x 10^{-4} mol., 4 eq.) and DIPEA (86 µL, 4.96 x 10^{-4} mol., 8 eq.) were used following the general procedure described above. The obtained yield is 89% (0.365 g, 5.52 x 10^{-5} mol.) as yellow translucent flakes. ^{1}H NMR (400 MHz, $CDCl_3$) δ 8.24 – 8.12 (m, 8H), 7.90 (s, 8H), 7.54 (d, J = 6.4 Hz, 16H), 7.07 (m, 136H), 4.74 (m, 12H), 4.40 (m, 68H), 4.00 – 3.57 (m, 92H), ^{13}C NMR (400 MHz, $CDCl_3$) δ 177.82 (s), 143.58 (s), 141.31 (s), 131.77 (s), 131.29 (s), 128.07 – 127.51 (m), 126.52 (s), 124.95 (s), 68.47 (t, J = 47.0 Hz), 63.76 (s), 29.70 (s), 27.81 (s), 25.61 (s), 22.18 (s). IR (NaCl): 3138, 2924 (t), 1950, 1736, 1555, 1461, 1346, 1205, 1128, 1065, 1111, 756 ν cm^{-1}. HRMS: cald. 6558.94 found 6559.0

Synthesis of *l*-G3 (22)

EO3-EO2-G3-N_3 (**13**) (0.164 g, 3.31 x 10^{-5} mol., 1 eq.), compound **19** (0.285 g, 5.28 x 10^{-4} mol., 16 eq.), CuI (0.100 g, 5.28 x 10^{-4} mol., 16 eq.) and DIPEA (92 µL, 5.28 x 10^{-4} mol, 16 eq.) were used following the general procedure described above. The obtained yield is 75 % (0.337 g, 2.48 x 10^{-5} mol) as brown flakes. ^{1}H NMR (400 MHz, $CDCl_3$) δ 8.26 – 8.10 (m, 16H), 7.88 (br, 16H), 7.56 (d, J = 19.0 Hz, 32H), 7.19 – 6.91 (m, 272H), 4.74 (s, 24H), 4.49 (m, 136H), 3.98 – 3.60 (m, 204H). ^{13}C NMR (400 MHz, $CDCl_3$) δ 143.58 (s), 131.79 (s), 131.30 (s), 128.60 (s), 128.00 – 127.38 (m), 126.54 (s), 124.95 (s), 120.99 (s), 69.46 (s), 68.90 (s), 63.78 (s), 50.33 – 49.43 (m), 29.71 (s). IR (NaCl): 3142, 3053 (t), 2925 (br t), 1950, 1734, 1555, 1444, 1346, 1207, 1126, 1066, 910 ν cm^{-1}. HRMS: cald. 13589.2 found 13658.5 (M + Cu)

Synthesis of *l*-G4 (23)

EO3-EO2-G4-N_3 (**15**) (0.147 g, 1.41 x 10^{-5} mol., 1 eq.), compound **19** (0.244 g, 4.52 x 10^{-4} mol., 32 eq.), CuI (0.086 g, 4.52 x 10^{-4} mol., 32 eq.) and DIPEA (80 µL, 5.28 x 10^{-4} mol., 3 eq.) were used following the general procedure described above. The obtained yield is 71% (0.136 g, 1.00 x 10^{-5} mol.) as pale yellow flakes. ^{1}H NMR (400 MHz, $CDCl_3$) δ 8.19 (m, 32H), 7.90 (s, 32H), 7.53 (d, J = 7.3 Hz, 64H), 7.07 (m, 544H), 4.74 (br s, 48H), 4.63 – 4.25 (m, 272H), 3.99 – 3.59 (m, 424H). ^{13}C NMR (400 MHz, $CDCl_3$) δ 143.56 (s), 131.77 (s), 131.29 (s), 128.07 – 127.51 (m), 126.52 (s), 124.95 (s), 68.92 (s), 67.98 (s), 50.25 (s), 25.62 (s). IR (NaCl): 3142, 3053 (t), 2918 (br t), 2106, 1950, 1734, 1555, 1444, 1344, 1205, 1124, 1066, 1043 ν cm^{-1}. HRMS: Could not be obtained due to the limitation of our apparatus.

RESULTS AND DISCUSSION

Synthesis

The first step towards our objective was to synthesize the dendritic cores. The EO3-EO2 architecture described in the previous section was reproduced using its original procedure as shown in Scheme 2. It involves a copper-free cyclo-addition between a highly activated branching synthon (**7**) and the azide terminal points of the previous generation. The reaction is very efficient and generation growth can be realized with a precise ratio of 1 : 1 of synthon per terminal point. Synthesis of the core up to generation three was reported[32] and we applied their procedure to create generation four. Its transformation (**14**) and subsequent activation into azide (**15**)

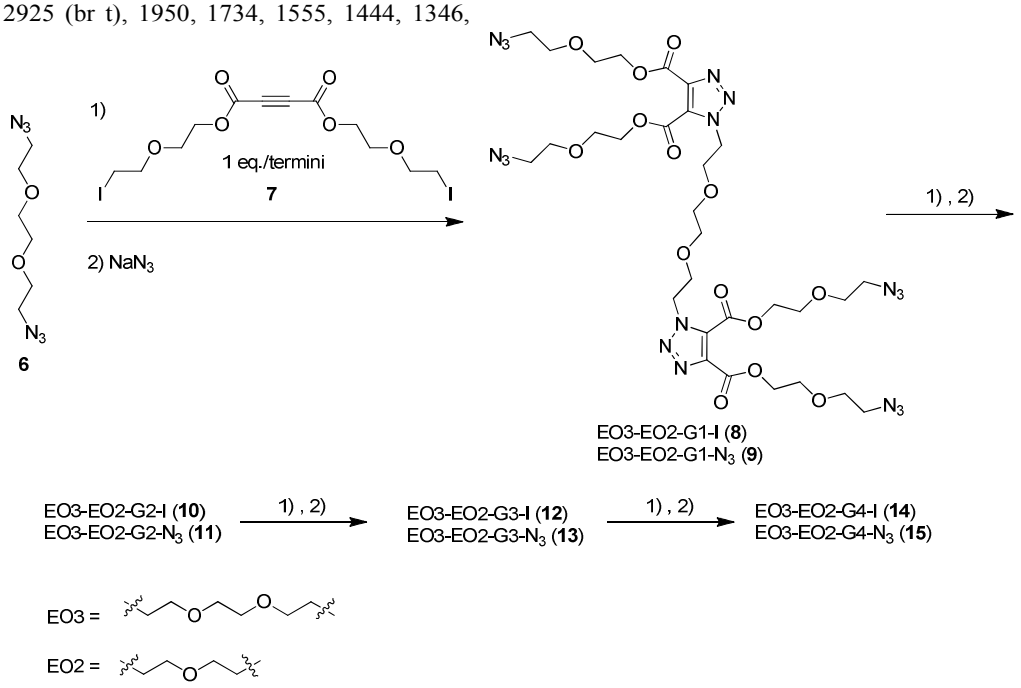

Scheme 2 The synthetic route to build the EO2-EO3 dendritic core.

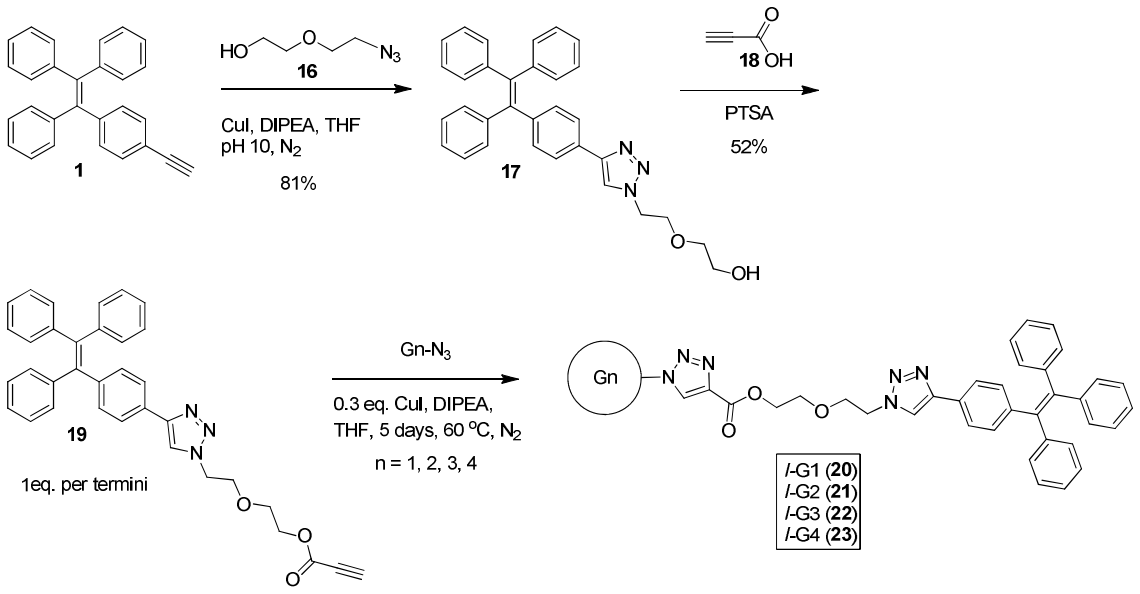

Scheme 3 The alternative strategy route leading to the "long" (l) dendrimers series.

were completed efficiently and were monitored mainly by ^{1}H NMR with the methylene next to the termini and by infrared through the azide band (2095-2100 cm^{-1}). The long aliphatic branches of this dendrimer are well suited for a CuAAC[34] by minimizing steric hindrance at the site of reaction. Despite its high efficiency, click chemistry applied onto macromolecules can be incomplete mainly due to acute steric hindrance and the added difficulty of conducting many reactions at once on the same substrate.[35, 36] Therefore, we first investigated the methodology pictured in Scheme 1 with the naked EO3 core (**6**) to synthesize G0 (**2**). TPE-alkyne (1) was synthesized through reported means with similar yields.[25] Because TPE is hydrophobic, we chose suitable conditions over the hydrophilic classic ones. Copper iodide in THF with triethylamine was used at room temperature. This less-than-quantitative result suggested that decorating higher generations with TPE would not be as straightforward as one would think. Indeed, the final conditions we used are deviating considerably from the standard CuAAC.[34]

As shown in Scheme 1, heat, extensive reaction times and a high excess of TPE were needed.Each of the dendrimer (G0 to *s*-G3) was fully characterized by NMR, IR and mass spectrometry (MS). Similar to the core synthesis, monitoring the azide band in IR proved to be the best tool to assess the completion of the decoration as presented in Figure 2. Generation 1, 2, and 3 were obtained this way, but purification of *s*-G3 (**5**) resulted in a 9 % yield. The same procedure was applied to the G4 dendrimer core (**15**), but despite our best efforts, the target molecule was never obtained.

From there, a strategy involving click-activating spacer was devised. It involved the synthesis of TPE-EO alcohol (**17**) that would then be linked to propiolic acid to yield compound **19** (Scheme 3). A CuAAC was then performed with G1, 2, 3 and 4 in the same conditions developed above except that a 1:1 ratio between **19** and the dendrimers termini was used.

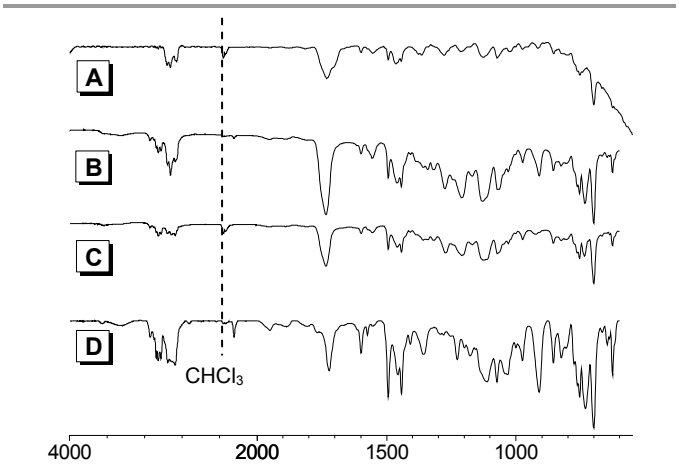

Fig. 2 Infrared spectra for s-G3 (A), s-G2 (B), s-G1 (C) and G0 (D).

The only purification needed were the ammonium chloride washes to remove copper. Fully functionalized dendrimers were collected in each case except for G4. *l*-G4 showed complete transformation through ^{1}H NMR (see SI, Figure S1), but a very small peak corresponding to the unreacted azide termini can be seen in IR (Figure 3, 2100 cm^{-1}). The combination of these two characterization techniques points to a conversion rate of about 95 %. By thin layer chromatography (TLC), ^{1}H NMR and IR, no leftover unreacted alkyne-TPE (**19**) can be observed. Despite this limitation, a massive dendrimer with a polydispersity of 1.03 (determined by size exclusion chromatography) was obtained. Combined with the first dendrimers, this new strategy yielded two distinct series of molecules with a different architecture at their periphery. The first series is labelled as "short" (*s*) while the one prepared through the second strategy is called "long" (*l*) as there are

more sigma bonds from the terminal TPE to the first branching point in the dendrimer core (Figure 4).

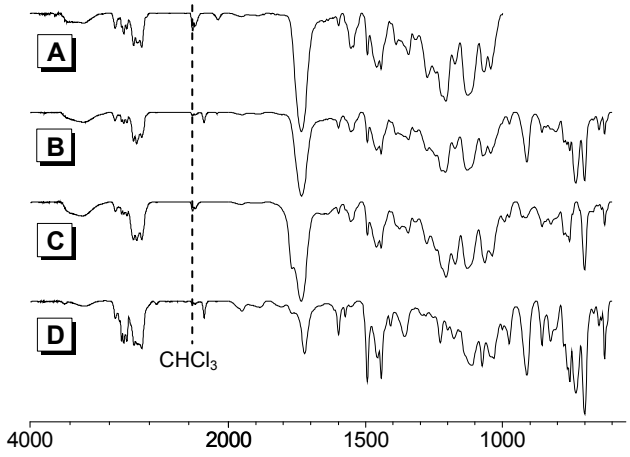

Fig. 3 Infrared spectra for l-G4 (A), l-G3 (B), l-G2 (C) and l-G1 (D).

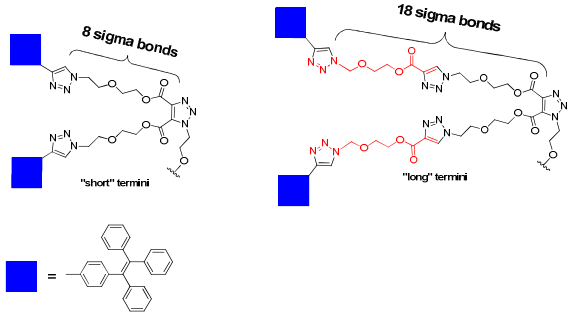

Fig. 4 Comparison between the "short" and the "long" termini.

Photoluminescence Studies

The first way to test whether a compound is AIE or not is to confirm its solid-state emission. Because of the EO branches flexibility, the dendrimers do not crystallize properly but instead form a flaky yellow solid when dried. All of them are emissive when exposed to UV (see fig. S12 for an example). With both series of dendrimers in hand, their emission behaviour was investigated through the typical AIE experiment. This is done by dissolving each dendrimer in pure THF and then adding water as a bad solvent. At every increment of water fraction (f_w), the emission spectrum is collected. All *f* values are volume/volume percentages. Because the substrate is fully solvated in THF, it does not emit. When enough water is added to the mixture, the dendrimer will start aggregating. In these aggregates, the TPE units are restrained and start emitting. Taking *l*-G4 (**23**) as an example, Figure 5 shows the typical result from this technique: as the water fraction increases the emission intensity increases as well. Figure 5 (C) shows a photo of the dendrimers at the 95 % f_w under UV lamp excitation. All eight dendrimers exhibit this typical AIE behaviour except for

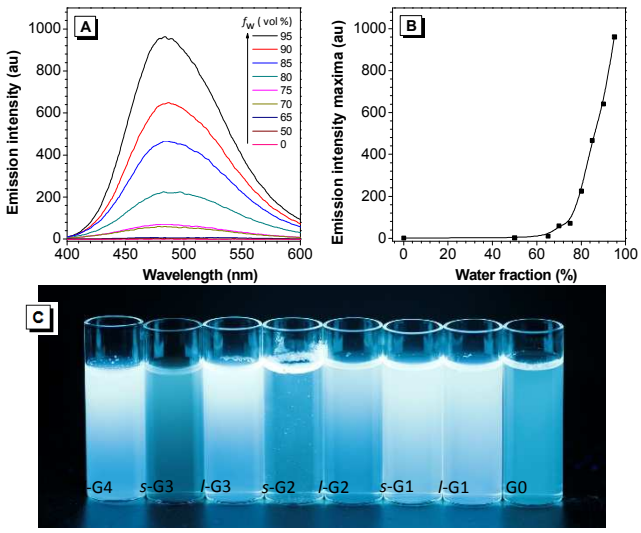

Fig. 5 Emission spectra of l-G4 (23) in THF–water mixtures. (A) Plot of intensity values versus the compositions of the aqueous mixtures. Solution concentration: 10^{-5} M; excitation wavelength: 327 nm. (B) Photo of the dendrimers under UV lamp excitation at 95 % fw (C).

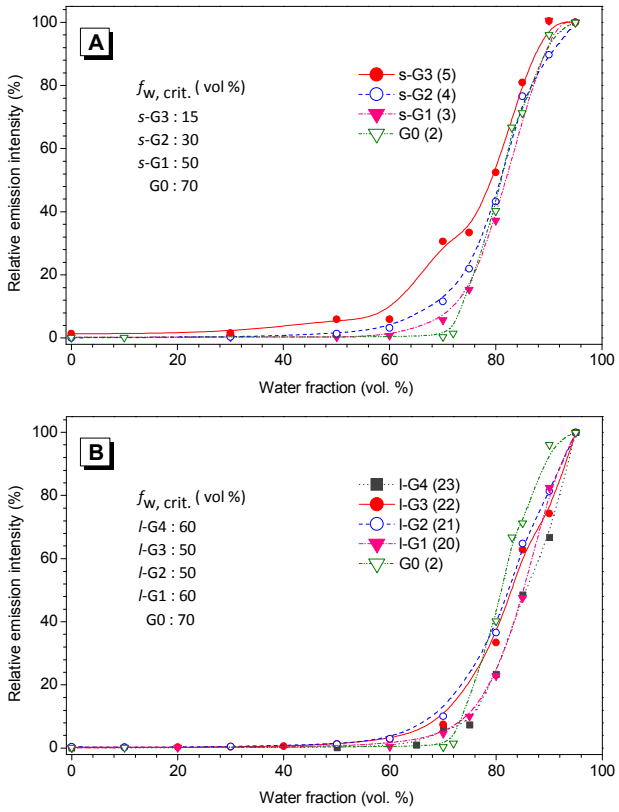

Fig. 6 Plot of the relative intensity (%) values versus the compositions of the aqueous mixtures for the short dendrimers (A) and for the long ones (B), including G0 for both. Concentration for all samples was 10^{-5} M.

s-G3 (**5**), which has a slim background emission in pure THF as seen in Figure 6A (red curve). This result indicates that

peripheral crowding start occurring at the third generation, confirming our hypothesis.

AIE is a complex, multidimensional phenomenon and it can be used and analysed several ways to gather more information. One way to do so is to normalize the intensity maximum as a function of the f_w of each dendrimer to better compare them to each other. Figure 6 collects the results from the "short" series in panel A and those from the "long" series in panel B. There is a clear trend for the "short" series where the mixture needs less and less water to start emitting as the dendrimer generation increase from 0 to 3. This value, abbreviated $f_{w\ crit.}$ for critical water fraction, represents the critical points at which the substrates start emitting. Indeed, G0 aggregates start emitting at 70 % f_w while *s*-G1 (**3**) starts to emit at 50 % f_w and *s*-G2 (**4**) starts at 30 % f_w. Meanwhile, *s*-G3 (**5**) is not only emissive from 0 % f_w, but its emission intensity also climbs much sooner (15 % f_w). This is most likely due to the fact that as the generation grows, the dendrimer grows less tolerant of water, and therefore is more prone to aggregation. The "long" series does not exhibit the same trend between the generations. This difference comes from the rotational freedom added by the EO spacer. Each "long" generation is free to re-arrange itself in its own way. This difference between the "short" and the "long" ones is an indication that AIE can be very sensitive to relatively small, yet crucial, changes in a macromolecular architecture and conformation.

Another noteworthy point that can be derived from the raw emission intensity is the increase of intensity from the dilute solution (I_0) to the aggregated state (I). The measurement of I/I_0 gives an assessment of the AIE relative strength for a given molecule. In the case of our dendrimers, each of them shows an I/I_0 nearing three orders of magnitude which is higher what was observed by Tanaka *et al* (I/I_0 of 70).[19]

To further compare the emission of our substrates, we performed the AIE experiment described above again, only this time, using the 95 % f_w of each dendrimer series at 10^{-5} M and a fixed setting on our apparatus. Our initial thought was that a power 2 exponential upward trend would be observed corresponding to the increase of the absolute quantity of TPE units present in the sample. This would have meant that the dendritic architecture has little to no influence on the emission intensity of the aggregates. This was not the case. Whether the molar concentration or the TPE concentration was kept constant, no clear trend was observed for both the long and the short series (see Figure S3). The ethylene oxide core probably acts as a deformable sponge, preventing efficient packing inside the aggregates. This leads to a decrease of emission intensity. The ratio of TPE units per molar mass of EO branches gives each generation a unique situation that, in turn, leads to a unique emission efficiency. This is in accordance with previous reports arguing that, from low to high generations, dendrimers go through various domains of behaviour.[37] Nevertheless, this result further demonstrates the sensitivity of AIE when used as structural probe.

An alternative explanation to peripheral crowding would be the presence of backfolding. In such case, the TPE units would hide inside the dendritic core. The steric pressure would then trigger the fluorescence emission. The addition of water would also exacerbate the phenomenon. Yet, this is unlikely since the "long" series would show some emission in pure THF since they have the most flexible arms, especially at G4. The current research is complementary to that of the community of researchers who use pyrene excimer/exciplex interactions to investigate similar issues.[38] The TPE fluorescence can interact with anything surrounding it and is not sensitive to a specific orientation. Therefore, the method presented here does not require complex mathematical treatment. It can be applied to a different range of experimental setups, providing information of an entire system instead of the orientation of two isolated moieties in respect to each other.

Dynamic Light Scattering (DLS) Studies

To further investigate the relationship between the aggregates and their emission, DLS was used. First, the size of each dendrimer was measured in pure THF at the 2 x 10^{-5} M concentration. All of them display a radius close to their calculated one. This indicates that they are fully dissociated in pure THF. We then investigated the relationship between the size of the aggregates and their emission. To do so, every increment of the typical AIE experiment was used for a DLS measurement right after the emission spectrum was gathered.

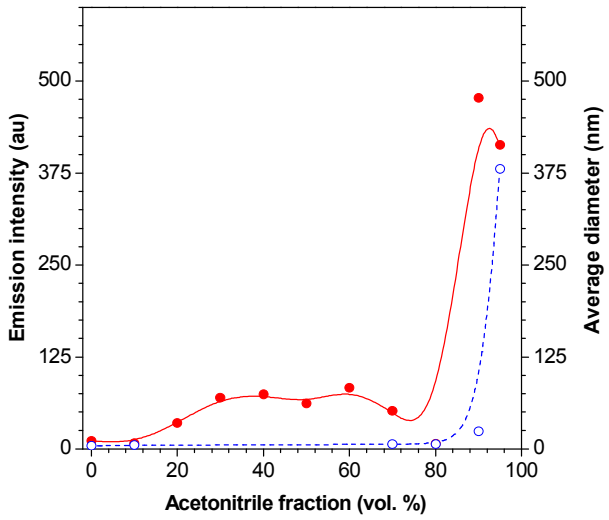

Fig. 7 Average diameter for particles observed in DLS (red full line) and the emission intensity (blue dashed line) as a function of the acetonitrile fraction against THF for l-G4 (23). Concentration is 10^{-5} M.

l-G4 (**23**) was selected for this because it shows the most intense emission. Water could not be used as the bad solvent

here since the aggregates were not only too big, but also had such a wide polydispersity that the results would have been impossible to interpret with DLS. Since the aggregates formed during this experiment constitute a metastable precipitate, a solvent with some hydrophobicity that retains partial hydrophilicity would lead to a milder precipitation made of smaller aggregates, enabling DLS measurements. Acetonitrile (ACN) was selected as a replacement bad solvent. It is amphiphilic and the selected dendrimer is insoluble in it. Figure 7 shows the resulting combined graphic. As was predicted, $f_{ACN\ crit.}$ is higher than $f_{w\ crit}$, confirming that ACN is a milder bad solvent to which *l*-G4 (**23**) is more tolerant. It also reveals two distinct regimes of aggregation. The first one occurs from 20 % to 80 % f_{ACN}. It features small aggregates that do not emit, most likely because they are too loose. The aggregates of the second regime (80% and up) are much larger than those of the first regime and most importantly, are emissive. The size of these aggregates seems to correlate with the emission intensity, up to 90 % f_{ACN} where they shrink by about 100 nm while the emission keeps rising. This shows that the aggregates emission is dictated not only its size but also by its compactness.

Conclusion

In the present paper we reported the synthesis of large AIE-active dendrimers. Several difficulties were encountered and harsh CuAAC conditions were necessary in order to decorate them. To circumvent this and reach G4, a click-activating spacer was created. It yielded AIE-active dendrimers with the highest molar weight so far to the best of our knowledge. As shown by various characterization techniques, their decoration is near complete all the way to G4 with excellent monodispersity. We successfully demonstrated that the architectural changes that come with each new generation can be distinguished using the standard AIE experiment. The measurements showed that peripheral crowding starts at the third generation. Going even further, the technique is able to differentiate subtle changes in architecture as seen with the "long" and "short" series. It also revealed that each generation behaves on its own due to a varying hydrophilicity. The synergy between AIE and DLS revealed a complex relationship between the aggregates size and their emission. This opened up a new avenue for us and we are actively looking into this. The high sensitivity of AIE to both internal factors (architecture) and external stimuli (solvent changes) gives it a place of choice in investigating biomolecular phenomenon that occur over large systems like the fluorescence emission of jellyfish breathing.

ACKNOWLEDGMENT

This work reported in this paper was partially supported by the National Basic Research Program of China (973 Program; 2013CB834701), the RPC and SRFI Grants of HKUST (RPC11SC09 and SRFI11SC03PG), the Research Grants Council of Hong Kong (HKUST2/CRF/10 and N-HKUST620/11), and the University Grants Committee of Hong Kong (AoE/P-03/08). B. Z. Tang thanks the support of the Guangdong Innovative Research Team Program (201101C0105067115).

REFERENCES

1. J. D. Luo, Z. L. Xie, J. W. Y. Lam, L. Cheng, H. Y. Chen, C. F. Qiu, H. S. Kwok, X. W. Zhan, Y. Q. Liu, D. B. Zhu and B. Z. Tang, *Chem Commun*, 2001, 1740-1741.
2. G. v. Bünau, *Berichte der Bunsengesellschaft für physikalische Chemie*, 1970, **74**, 1294-1295.
3. T. Förster and K. Kasper, *Z. Phys. Chem. (Munich)*, 1954, **1**, 275.
4. J. L. Robeson and R. D. Tilton, *Biophys J*, 1995, **68**, 2145-2155.
5. X.-H. Zhu, J. Peng, Y. Cao and J. Roncali, *Chem Soc Rev*, 2011, **40**, 3509-3524.
6. M. Vendrell, D. Zhai, J. C. Er and Y.-T. Chang, *Chem Rev*, 2012, **112**, 4391-4420.
7. A. Herrmann, T. Weil, V. Sinigersky, U.-M. Wiesler, T. Vosch, J. Hofkens, F. C. De Schryver and K. Müllen, *Chem. Eur. J.*, 2001, **7**, 4844-4853.
8. H. Xiao, K. Chen, D. Cui, N. Jiang, G. Yin, J. Wang and R.-Y. Wang, *New J Chem*, 2014.
9. V. Bhalla, S. Pramanik and M. Kumar, *Chem Commun*, 2013, **49**, 895-897.
10. Y. N. Hong, J. W. Y. Lam and B. Z. Tang, *Chem Commun*, 2009, 4332-4353.
11. Y. N. Hong, J. W. Y. Lam and B. Z. Tang, *Chem Soc Rev*, 2011, **40**, 5361-5388.
12. S. Zhang, A. J. Qin, J. Z. Sun and B. Z. Tang, *Prog Chem*, 2011, **23**, 623-636.
13. N. W. Tseng, J. Z. Liu, J. C. Y. Ng, J. W. Y. Lam, H. H. Y. Sung, I. D. Williams and B. Z. Tang, *Chem Sci*, 2012, **3**, 493-497.
14. J. Chen and B. Z. Tang, in *Aggregation-Induced Emission: Fundamentals and Applications, Volumes 1 and 2*, John Wiley and Sons Ltd, 2013, pp. 307-322.
15. D. A. Tomalia, H. Baker, J. Dewald, M. Hall, G. Kallos, S. Martin, J. Roeck, J. Ryder and P. Smith, *Polym J*, 1985, **17**, 117-132.
16. G. R. Newkome, C. N. Moorefield and F. Vögtle, in *Dendritic Molecules*, Wiley-VCH Verlag GmbH, 2007, pp. 1-13.
17. D. A. Tomalia and J. M. J. Fréchet, in *Dendrimers and Other Dendritic Polymers*, John Wiley & Sons, Ltd, 2002, pp. 1-44.
18. R. Dong, B. Zhu, Y. Zhou, D. Yan and X. Zhu, *Angew. Chem. Int. Ed.*, 2012, **51**, 11633-11637.
19. K. Shiraishi, T. Kashiwabara, T. Sanji and M. Tanaka, *New J Chem*, 2009, **33**, 1680-1684.
20. G. X. Huang, B. D. Ma, J. M. Chen, Q. Peng, G. X. Zhang, Q. H. Fan and D. Q. Zhang, *Chem-Eur J*, 2012, **18**, 3886-3892.
21. D. F. Xu, X. L. Liu, R. Lu, P. C. Xue, X. F. Zhang, H. P. Zhou and J. H. Jia, *Org Biomol Chem*, 2011, **9**, 1523-1528.

22. M. K. Leung, Y. S. Lin, C. C. Lee, C. C. Chang, Y. X. Wang, C. P. Kuo, N. Singh, K. R. Lin, C. W. Hu, C. Y. Tseng and K. C. Ho, *Rsc Adv*, 2013, **3**, 22219-22228.
23. Y. H. Jiang, Y. C. Wang, J. L. Hua, J. Tang, B. Li, S. X. Qian and H. Tian, *Chem Commun*, 2010, **46**, 4689-4691.
24. B. Xu, J. Zhang, H. Fang, S. Ma, Q. Chen, H. Sun, C. Im and W. Tian, *Polym Chem-Uk*, 2014.
25. J. Wang, J. Mei, E. G. Zhao, Z. G. Song, A. J. Qin, J. Z. Sun and B. Z. Tang, *Macromol.*, 2012, **45**, 7692-7703.
26. J. Z. Liu, Y. C. Zhong, J. W. Y. Lam, P. Lu, Y. N. Hong, Y. Yu, Y. N. Yue, M. Faisal, H. H. Y. Sung, I. D. Williams, K. S. Wong and B. Z. Tang, *Macromol.*, 2010, **43**, 4921-4936.
27. J. Wang, J. Mei, W. Z. Yuan, P. Lu, A. J. Qin, J. Z. Sun, Y. G. Ma and B. Z. Tang, *J Mater Chem*, 2011, **21**, 4056-4059.
28. R. R. Hu, J. W. Y. Lam, J. Z. Liu, H. H. Y. Sung, I. D. Williams, Z. N. Yue, K. S. Wong, M. M. F. Yuen and B. Z. Tang, *Polym Chem-Uk*, 2012, **3**, 1481-1489.
29. L. P. Heng, W. Qin, S. J. Chen, R. R. Hu, J. Li, N. Zhao, S. T. Wang, B. Z. Tang and L. Jiang, *J Mater Chem*, 2012, **22**, 15869-15873.
30. H. K. Li, H. Q. Wu, E. G. Zhao, J. Li, J. Z. Sun, A. J. Qin and B. Z. Tang, *Macromol.*, 2013, **46**, 3907-3914.
31. Q. Wang, M. Chen, B. C. Yao, J. Wang, J. Mei, J. Z. Sun, A. J. Qin and B. Z. Tang, *Macromol Rapid Comm*, 2013, **34**, 796-802.
32. M. Arseneault, I. Levesque and J. F. Morin, *Macromol.*, 2012, **45**, 3687-3694.
33. V. Aucagne, I. E. Valverde, P. Marceau, M. Galibert, N. Dendane and A. F. Delmas, *Angew. Chem. Int. Ed.*, 2012, **51**, 11320-11324.
34. H. C. Kolb, M. G. Finn and K. B. Sharpless, *Angew. Chem. Int. Ed.*, 2001, **40**, 2004-2021.
35. M. Arseneault, P. Dufour, I. Levesque and J.-F. Morin, *Polym Chem-Uk*, 2011, **2**, 2293-2298.
36. G. Franc and A. Kakkar, *Chem Commun*, 2008, 5267-5276.
37. S. Mignani and J.-P. Majoral, *New J Chem*, 2013, **37**, 3337-3357.
38. J. Duhamel, *Polymers-Basel*, 2012, **4**, 211-239.